Refrigerant capacity of austenite in as-quenched and annealed $Ni_{51.1}Mn_{31.2}In_{17.7}$ melt spun ribbons

J. L. Sánchez Llamazares, H. Flores-Zuñiga, C. Sánchez-Valdes, C. A. Ross, and C. García

Citation: Journal of Applied Physics **111**, 07A932 (2012);
View online: https://doi.org/10.1063/1.3676606
View Table of Contents: http://aip.scitation.org/toc/jap/111/7
Published by the American Institute of Physics

Refrigerant capacity of austenite in as-quenched and annealed $Ni_{51.1}Mn_{31.2}In_{17.7}$ melt spun ribbons

J. L. Sánchez Llamazares,[1,a)] H. Flores-Zuñiga,[1] C. Sánchez-Valdes,[2] C. A. Ross,[3] and C. García[3,4]
[1]*Instituto Potosino de Investigación Científica y Tecnológica, Camino a la Presa San José 2055 Col. Lomas 4ª, San Luis Potosí, S.L.P. 78216, Mexico*
[2]*Institut de Ciencia de Materials de Barcelona (C.S.I.C.), Campus U.A.B., 08193 Bellaterra, Spain*
[3]*Department of Materials Science and Engineering, Massachusetts Institute of Technology, Cambridge, Massachusetts 02139, USA*
[4]*Physics Department, Bogaziçi University, North Campus KB 331-O, Bebek/Istanbul, Turkey*

(Presented 31 October 2011; received 23 September 2011; accepted 11 November 2011; published online 7 March 2012)

The thermal dependence of the magnetic entropy change ($\Delta S_M(T)$) and refrigerant capacity (*RC*) of austenite in as-quenched ribbons of chemical composition $Ni_{51.1}Mn_{31.2}In_{17.7}$ produced by melt spinning at a high cooling rate of 48 ms^{-1} is reported. The effect of annealing at 1073 K on the structure and the magnetic properties was studied. The as-quenched sample is a single-phase austenite that presents a B2 ordered structure. The annealing on the melt spun samples produced a $L2_1$-type ordered structure. Austenite is characterized by a broad $\Delta S_M(T)$ curve that, for a field change of 5.0 T, exhibits a full-width at half-maximum δT_{FMHW} of 107 K, a peak value of the magnetic entropy change ΔS_M^{peak} of -3.1 Jkg^{-1} K^{-1}, and $RC = 345$ Jkg^{-1}. Although annealed samples show larger ΔS_M^{peak} values the narrower $\Delta S_M(T)$ curves leads to a reduction in *RC*. Thus, the as-quenched sample shows a higher efficiency for a refrigerant cycle. © *2012 American Institute of Physics*. [doi:10.1063/1.3676606]

I. INTRODUCTION

The refrigerant capacity (*RC*) of magneto-caloric materials is, together with the peak magnetic entropy change (ΔS_M^{peak}), and the adiabatic temperature change (ΔT_{ad}), one of the three main figures of merit that allow the evaluation and comparison of their quality as coolants for magnetic refrigeration.[1] *RC* measures the amount of heat that can be transferred between the hot and cold sinks when an ideal thermodynamic cycle is considered. It is estimated from the thermal dependence of the magnetic entropy change ($\Delta S_M(T)$) by the three following methods: (a) Finding the product $\Delta S_M^{peak} \times \delta T_{FWHM}$ (hereafter referred to as *RC-1*), where $\delta T_{FWHM} = T_{hot} - T_{cold}$ is the temperature range that corresponds to the full width at half maximum of the $\Delta S_M(T)$ curve.[1] Here, δT_{FWHM} coincides with the temperature span of the thermodynamic cycle; (b) by calculating the integral, $\int_{T_{hot}}^{T_{cold}} [\Delta S_M(T)]_{\Delta H} dT$ (hereafter referred to as *RC-2*),[2] and; (c) maximizing the product $\Delta S_M \times \delta T$ below the $\Delta S_M(T)$ curve (referred as *RC-3*).[3] Hence, the expansion of δT, which is equivalent to the broadening in the $\Delta S_M(T)$ curve, is an effective way to enhance *RC*.

In recent years, considerable attention has been devoted to investigating the magneto-caloric properties of Heusler-type ferromagnetic shape memory alloys in the ternary system $Ni_{50}Mn_{50-x}In_x$ (i.e., with $15 \leq x \leq 16$).[4–10] These materials exhibit both, inverse and direct magneto-caloric effects associated with the magnetization change (ΔM) caused by the first-order structural martensite to austenite phase transition and the second-order magnetic transition of austenite, respectively. Nevertheless, it has been stated that despite the superior absolute value of the ΔS_M^{peak} obtained when the reverse martensitic transformation occurs with respect to that obtained around the ferromagnetic transition of austenite, the large hysteresis losses due to the effect of the magnetic field on the phase transformation as well as the narrower $\Delta S_M(T)$ curve make the temperature interval around the ferromagnetic transition of austenite possess a higher *RC*.[6,10] In a different composition range, namely, $16 < x \leq 20$, the crystalline phase that forms in $Ni_{50}Mn_{50-x}In_x$ alloys is a ferromagnetic austenite that exhibits a high spontaneous magnetization and a Curie temperature T_C that lies around room temperature and is weakly dependent on the chemical composition.[11,12] In this work, we fabricated austenitic Ni-Mn-In alloy ribbons and investigated the effect of annealing at 1073 K on the magnetic entropy change and RC. The average chemical composition of the as determined by energy dispersive spectroscopy, was $Ni_{51.1}Mn_{31.2}In_{17.7}$. We show that the broadening of the $\Delta S_M(T)$ curve due to the characteristic chemical and crystal disorder induced by the quick transition from the liquid to the solid state leads to a considerable *RC* enhancement.

II. EXPERIMENTAL PROCEDURES

Polycrystalline alloy ribbons were prepared by melt spinning at a high wheel speed of 48 ms^{-1} (sample A). A detailed description of the experimental procedure is given in Refs. 13 and 14. Ribbon flakes were wrapped in Ta foils, sealed in high vacuum quartz ampoules, and annealed at 1073 K during 10 min (sample B), and 2 h (sample C), and then quenched in water.

X-ray diffraction (XRD) analyses were performed on powdered samples in a Bruker AXS model D8 Advance X-ray

a)Author to whom correspondence should be addressed. Electronic mail: sanchez@nanomagnetics.org.

powder diffractometer with Cu-Kα radiation ($\lambda = 1.5418$ Å). Scanning was carried out in the interval $10^o \leq 2\theta \leq 90^\circ$ with a step increment of 0.02°. Magnetization (M) measurements were performed by vibrating sample magnetometry in a Quantum Design PPMS® EverCool®-9 T platform. The magnetic field $\mu_o H$ was applied along the ribbon axis (i.e., rolling direction) to minimize the effect of the demagnetizing field. Magnetization as a function of temperature $M(T)$ curves was recorded at 2 K/min under an applied magnetic field of 5.0 mT. $\Delta S_M(T)$ curves were obtained by numerical integration of the Maxwell relation from a set of isothermal magnetization curves $M(H)$ measured from 188 to 328 K (in temperature step increments of $\Delta T = 4$ K), up to a maximum applied magnetic field of $\mu_o H_{max} = 5.0$ T.

III. RESULTS AND DISCUSSION

Figure 1(a) shows the room temperature XRD pattern of sample A. The diffraction peaks were indexed on the basis of an ordered B2 structure (CsCl-type). However, a low intensity and broad diffraction peak occurred at $2\theta \approx 25.7^\circ$, suggesting that a small volume fraction of the sample shows a $L2_1$-type crystalline order. Consequently, the dominant chemical order found in the as-quenched samples is that of B2. The inset in Fig. 1(a) shows the XRD peaks in the angle interval $22^o < 2\theta \leq 36^\circ$ for samples A, B, and C. After annealing, the (111) reflection of the $L2_1$ structure is clearly defined. In view of that, the crystal structure of samples B and C was identified as a highly ordered $L2_1$-type with lattice parameter $a = 0.59862$ nm, and $a = 0.59843$ nm, respectively. The reduction of the lattice constant with the increase of the annealing time indicates progressive improvement of the crystalline ordering. No traces of secondary phases were observed in the diffractograms.

Figure 1(b) shows the $M(T)$ curves obtained under low and high applied magnetic field values of 5.0 mT (open symbols), and 5.0 T (closed symbols), respectively. The Curie point for sample A was 276 K, while for both samples B and C, $T_C = 288$ K. Therefore, the structural modification induced by the thermal annealing from B2 to the $L2_1$-type structure is accompanied by little change in the magnetic ordering temperature of austenite. In agreement with the increasing of the chemical order, the low-field $M(T)$ curves for annealed samples show a more abrupt drop of magnetization near T_C. The inset of Fig. 1(b) shows the normalized dM/dT versus T/T_C curves for samples A and C in order to draw attention to the fact that the main difference between both curves occurs in the ferromagnetic temperature region, namely, for $T < T_C$, which is attributed to the lower chemical order of austenite. This suggests a picture in which a broad distribution of T_C values arises as a consequence of the chemical disorder that characterizes the B2 structure. Upon annealing, samples show a noticeable increase in the saturation magnetization values. Its relative variation $\Delta M_S/M_S$ at 5.0 T and $T/T_C \approx 0.7$ was ~ 9 and 18% for samples B and C, respectively. This effect suggests the reinforcement of ferromagnetic exchange interactions between Mn atoms due to the modification of the configuration of neighboring atoms and interatomic distances between them.

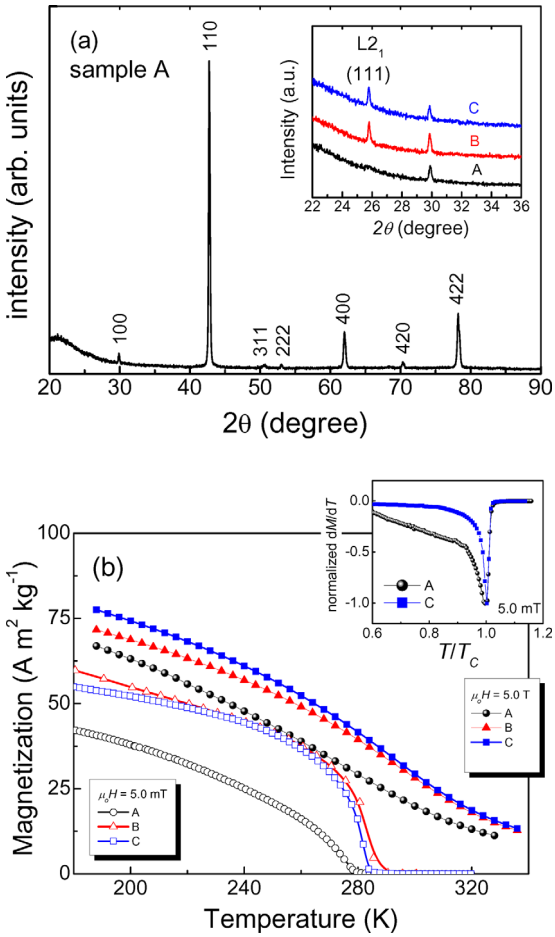

FIG. 1. (Color online) (a) Room temperature X-ray diffraction pattern for sample A. Inset: XRD patterns in the angle interval $22^o < 2\theta \leq 36^\circ$ for samples A, B, and C. (b) $M(T)$ curves measured in the field-cooled regime for the three samples studied at 5.0 mT (open symbols), and 5.0 T (full symbols). Inset: Normalized dM/dT vs T/T_C curves at 5.0 mT for samples A and C.

Figure 2(a) shows the $\Delta S_M(T)$ curves at 2.0 and 5.0 T, along with the curves $\left|\Delta S_M^{peak}\right|$ versus $(\mu_o H)^{2/3}$ (left inset), and $\Delta S_M(T)/\Delta S_M{}^{peak}$ versus T/T_C. At 5.0 T, the as-quenched sample shows a moderate absolute peak value of the magnetic entropy change of 3.1 Jkg^{-1} K^{-1}, along with a broad working temperature span δT_{FMHW} of 112 K. The left inset shows that $\left|\Delta S_M^{peak}\right|$ does not depend linearly on $(\mu_o H)^{2/3}$, a fact that could be related to the broad distribution of T_C values mentioned above (for further discussion, see Ref. 15). Further evidence is given in the right inset of Fig. 2(a) where we plot the normalized $\Delta S_M(T)/\Delta S_M{}^{peak}$ versus T/T_C curves. For samples B and C the curves overlap in the whole temperature range, while that of sample A visibly splits below T_C (i.e., in the ferromagnetic temperature region). On the contrary, the annealed samples B and C exhibit a narrower $\Delta S_M(T)$ curve with a similar value of $\left|\Delta S_M^{peak}\right|$ (4.1 and 4.4 Jkg^{-1} K-1, respectively), and δT_{FMHW} values of 65 and 67 K, respectively. Also for samples B and C $\left|\Delta S_M^{max}\right|$ is proportional to $(\mu_o H)^{2/3}$, a dependence that is satisfied by many ferromagnets with second-order magnetic transition.[1,15]

Figure 2(b) compares for samples A and B, the field dependence of both, *RC-2* and the characteristic temperatures, T_{hot} and T_{cold}, that define the full-width at half-maximum of the

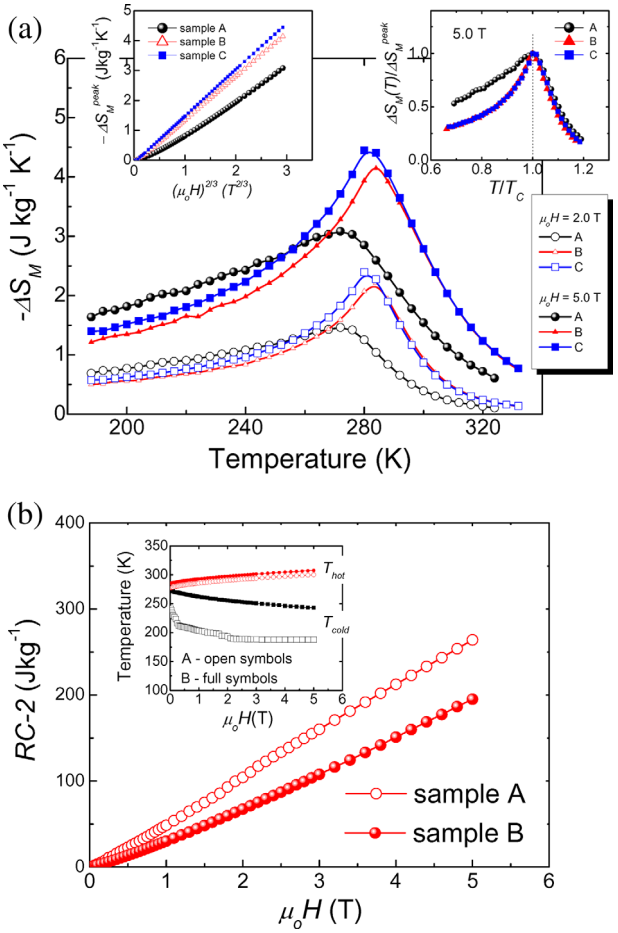

FIG. 2. (Color online) (a) Thermal dependence of the magnetic entropy change $\Delta S_M(T)$ at $\mu_o H = 2.0$ and 5.0 T, and ΔS_M^{peak} as a function of $(\mu_o H)^{2/3}$ (left inset) for samples A, B, and C. Right inset: $\Delta S_M(T)/\Delta S_M^{peak}$ vs T/T_C curve. (b) Field dependence of *RC-2* for samples A and B. Inset: Field dependence of the temperatures T_{hot} and T_{cold}.

$\Delta S_M(T)$ curve (see the inset). The increase of RC, due to the broadening of $\Delta S_M(T)$, is caused by the significant decrease in T_{cold} and the resulting 70% increase of δT_{FWHM} (as the inset shows) with respect to the δT_{FWHM} of the annealed samples.

Finally, a summary of the magneto-caloric properties at 2.0 and 5.0 T for the ribbons is given in Table I, in addition to the absolute value of ΔS_M^{peak}, *RC-1*, *RC-2*, and *RC-3* and the related temperature parameters. To put these results in context we can compare the *RC-2* values here obtained for sample A with those previously reported for bulk $Ni_{50}Mn_{50-x}In_x$ alloys with a similar T_C value by Pathak *et al.*[6] They found at $\mu o \Delta H_{max} = 5.0$ T, *RC-2* values between 240 and 280 Jkg^{-1} for $15.05 \leq x \leq 16$, which is similar to the one obtained here for as-quenched ribbons. However, likely that *RC* can be further improved by properly optimizing the chemical composition, or using appropriate additives.

IV. CONCLUSION

These results show that first, as-quenched rapidly solidified Ni-Mn-In alloy ribbons with the single-phase B2-type austenite show higher RC than those annealed at 1073 K where a highly ordered $L2_1$-type order is found. This is due to the broader $\Delta S_M(T)$ curve (i.e., the wider working temperature span δT_{FWHM} due to the decrease in T_{cold}). Hence, the use of high quenching rates from the melt enhances the RC of austenite via its structural modification. Second, the structural modification of austenite from a B2 to the $L2_1$-type is accompanied by a few degrees increase of T_C; a more abrupt fall of magnetization around T_C; a notable relative increase in the saturation magnetization; and a linear relationship between $\left|\Delta S_M^{peak}\right|$ and $(\mu_o H)^{2/3}$.

TABLE I. Summary of the magnetocaloric properties of samples A, B, and given for magnetic field changes $\mu_o \Delta H_{max}$ of 2.0 T and 5.0 T.

	Sample A		Sample B		Sample C	
	$\mu_o \Delta H_{max}$ (T)		$\mu_o \Delta H_{max}$ (T)		$\mu_o \Delta H_{max}$ (T)	
	2.0 T	5.0 T	2.0 T	5.0 T	2.0 T	5.0 T
$\lvert\Delta S_M^{peak}\rvert$ (Jkg^{-1}K^{-1})	1.4	3.1	2.2	4.1	2.4	4.4
RC-1	141	345	91	268	94	294
RC-2	103	264	67	195	74	216
δT_{FWHM} (K)	98	112	41	65	42	67
T_{hot} (K)	290	300	297	307	295	306
T_{cold} (K)	192	188	256	242	253	239
RC-3	73	182	62	162	67	180
δT^{RC-3} (K)	100	107	111	126	118	130
T_{hot} (K)[a]	290	297	307	319	306	317
T_{cold} (K)[a]	190	190	196	193	188	187

[a]Related to RC-3.

ACKNOWLEDGMENTS

The authors acknowledge financial support received from CONACYT, Mexico, under Projects CB-2010-01-156932 and 157541 and Laboratorio Nacional de Investigaciones en Nanociencias y Nanotecnología (LINAN, IPICyT). Technical support from M.Sc. G.J. Labrada-Delgado and B.A. Rivera-Escoto is recognized. C.F.S.V. thanks CSIC, Spain, for a Ph.D. grant (JAEPRE-08-00508).

[1]A. M. Tishin and Y. I. Spichkin, *The Magnetocaloric Effect and its Applications* (Institute of Physics, Bristol, 2003).
[2]K. A. Gschneidner, Jr., V. K. Pecharsky, A. O. Pecharsky, and C. B. Zimm, Mater. Sci. Forum **315**, 69 (1999).
[3]M. E. Wood and W. H. Potter, Cryogenics **25**, 667 (1985).
[4]Z. D. Han, D. H. Wang, C. L. Zhang, S. L. Tang, B. X. Gu, and Y. W. Du, Appl. Phys. Lett. **89**, 182507 (2006).
[5]T. Krenke, E. Duman, M. Acet, E. F. Wassermann, X. Moya, L. Mañosa, A. Planes, E. Suard, and B. Ouladdiaf, Phys. Rev. B **75**, 104414 (2007).
[6]A. K. Pathak, M. Khan, I. Dubenko, S. Stadler, and N. Ali, Appl. Phys. Lett. **90**, 262504 (2007).
[7]V. K. Sharma, M. K. Chattopadhyay, and S. B. Roy, J. Phys. D: Appl. Phys. **40**, 1869 (2007).
[8]X. Moya, L. Mañosa, A. Planes, S. Askoy, M. Acet, E. F. Wassermann, and T. Krenke, Phys. Rev. B **75**, 184412 (2007).
[9]M. K. Chattopadhyay, V. K. Sharma, and S. B. Roy, Appl. Phys. Lett. **92**, 022503 (2008).
[10]J. L. Sánchez Llamazares, C. García, B. Hernando, V. M. Prida, D. Baldomir, D. Serantes, and J. González, Appl. Phys. A, **103**, 1125 (2011).
[11]T. Krenke, M. Acet, E. F. Wassermann, X. Moya, L. Mañosa, and A. Planes, Phys. Rev. B **73**, 174413 (2006).
[12]R. Y. Umetsu, Y. Kusakari, T. Kanomata, K. Suga, Y. Sawai, K. Kindo, K. Oikawa, R. Kainuma, and K. Ishida, J. Phys. D: Appl. Phys. **42**, 075003 (2009).
[13]J. L. Sánchez Llamazares, T. Sanchez, J. D. Santos, M. J. Perez, M. L. Sanchez, B. Hernando, L. Escoda, J. J. Suñol, and R. Varga, Appl. Phys. Lett. **92**, 012513 (2008).
[14]J. L. Sánchez Llamazares, B. Hernando, C. García, J. González, Ll. Escoda, and J. J. Suñol, J. Phys. D: Appl. Phys. **42**, 045002 (2009).
[15]J. Lyubina, M. D. Kuz'min, K. Nenkov, O. Gutfleisch, M. Richter, D. L. Schlagel, T. A. Lograsso, and K. A. Gschneidner, Jr., Phys. Rev. B **83**, 012403 (2011).